Journal of Functional Foods 80 (2021) 104428

Contents lists available at ScienceDirect

Journal of Functional Foods

journal homepage: www.elsevier.com/locate/jff

Erythorbyl laurate suppresses TNF-α-induced adhesion of monocytes to the vascular endothelium

Su Jeong Ha [a,1], Min Jeong Kim [b,1], Joon Park [d,e], Hyun-Wook Choi [f], Hyunjong Yu [g,h], Pahn-Shick Chang [a,g,h,i,*], Sung Keun Jung [b,c,*]

[a] Department of Agricultural Biotechnology, Seoul National University, Seoul 08826, Republic of Korea
[b] School of Food Science and Biotechnology, Kyungpook National University, Daegu 41566, Republic of Korea
[c] Institute of Agricultural Science & Technology, Kyungpook National University, Daegu 41566, Republic of Korea
[d] Division of Food Functionality, Korea Food Research Institute, 245, Nongsaengmyeong-ro, Iseo-myeon, Wanju-gun, Jeollabuk-do 55365, Republic of Korea
[e] Department of Food Biotechnology, Korea University of Science & Technology, 217 Gajeong-ro, Yuseong-gu, Daejeon 34113, Republic of Korea
[f] Department of Functional Food and Biotechnology, Jeonju University, Jeonju 55069, Republic of Korea
[g] Center for Agricultural Microorganism and Enzyme, Seoul National University, Seoul 08826, Republic of Korea
[h] Research Institute of Agriculture and Life Sciences, Seoul National University, Seoul 08826, Republic of Korea
[i] Center for Food and Bioconvergence, Seoul National University, Seoul 08826, Republic of Korea

ARTICLE INFO

Keywords:
Erythorbyl laurate
Arteriosclerosis
Monocyte adhesion
Vascular inflammation
VCAM-1
NF-κB

ABSTRACT

Erythorbyl laurate (EL) can be produced via lipase-catalyzed esterification between erythorbic acid and lauric acid. In this study, we evaluate the anti-inflammatory effect of EL in the early stage of atherosclerosis. EL suppressed tumor necrosis factor (TNF)-α-induced monocyte adhesion to vascular endothelial cells and expression of vascular cell adhesion molecule (VCAM)-1 in human umbilical vein endothelial cells (HUVECs). Additionally, EL suppressed TNF-α-induced p65/IκB kinase (IKK)/IκB phosphorylation in HUVECs. Western blot analysis of cytosolic and nuclear cell fractions and immunofluorescence showed that EL suppressed TNF-α-induced translocation of p65 from the cytoplasm to the nucleus. EL also inhibited phosphorylation of extracellular-signal-regulated kinase (ERK) 1/2, p38, and c-Jun N-terminal kinases (JNK) 1/2 in HUVECs. EL suppressed TNF-α-induced phosphorylation of Akt, IRAK1, and TAK1 in HUVECs. Quantitative RT-PCR analysis showed that EL significantly suppressed TNF-α-induced interleukin *(IL)1B*, *IL6*, *TNFA*, and *CCL2* mRNA expression in HUVECs. Additionally, oral administration of EL suppressed TNF-α-induced IL6 and TNFA expression in the mouse aorta. EL could represent a promising functional nutrient that can be ingested for the prevention of vascular inflammation via decreased monocyte infiltration to the vascular endothelium and suppression of inflammatory nuclear factor (NF)-κB and mitogen-activated protein kinases (MAPKs) signaling pathways.

1. Introduction

Cardiovascular disease (CVD) represents an important health problem for modern aging societies, and remains the leading cause of morbidity and mortality in most Western countries (Sievenpiper & Lavie, 2018; Zimmer, Grebe, & Latz, 2015). Atherosclerosis, the underlying pathology of CVD, contributes to the development of heart attack and stroke, and is increasing worldwide in part due to the

Abbreviations: EL, Erythorbyl laurate; TNF-α, tumor necrosis factor; VCAM-1, vascular cell adhesion molecule; HUVEC, human umbilical vein endothelial cell; IKK, IκB kinase; ERK 1/2, extracellular-signal-regulated kinase 1/2; JNK, c-Jun N-terminal kinases 1/2; IL, interleukin; CCL2, monocyte chemoattractant protein-1; MAPK, mitogen-activated protein kinase; NF-κB, nuclear factor kappa-light-chain-enhancer of activated B cells; ABTS, 2,2′-azino-bis(3-ethylbenzothiazoline-6-sulfonic acid); DPPH, 1,1-Diphenyl-2-picrylhydrazyl; FBS, Fetal Bovine Serum; IRAK1, interleukin-1 receptor associated kinase 1; TAK1, transforming growth factor-β-activated kinase 1.

* Corresponding authors at: Department of Agricultural Biotechnology, Seoul National University, Seoul 08826, Republic of Korea (P.S. Chang). School of Food Science and Biotechnology, Kyungpook National University, Daegu 41566, Republic of Korea (S.K. Jung).
E-mail addresses: pschang@snu.ac.kr (P.-S. Chang), skjung04@knu.ac.kr (S.K. Jung).
[1] These authors have contributed equally to this work.

https://doi.org/10.1016/j.jff.2021.104428
Received 5 November 2020; Received in revised form 22 February 2021; Accepted 24 February 2021
Available online 21 March 2021

adoption of the Western lifestyle (Alwan, 2011; Hansson, 2005). Atherosclerosis can be divided into four stages: initiation, promotion, progression, and acute events (Kim & Jung, 2020). The early stages of atherosclerosis are characterized by the progressive accumulation of inflammatory cells such as monocyte into the intima, which consists of a single layer of endothelial cells and a subendothelial layer of collagen fibers of the arterial walls (Ha et al., 2018; Moss & Ramji, 2016a, 2016b). Accumulation of monocytes mainly occurs through monocyte capture by adhesion molecules expressed in neighboring endothelial cells. Thus, disruption of the interaction between monocytes and adhesion molecules by nutraceuticals could represent a promising strategy to prevent vascular inflammation and subsequent atherosclerosis.

Intracellular and intercellular communication via cell signaling maintains cellular homeostasis. When the environment of vascular cells changes due to the influx of cholesterol into blood vessels or an increase in inflammatory cytokines, intracellular signaling is also affected. Among the various molecules to provoke vascular inflammation, the transcription factor NF-κB has a critical role in inflammatory signaling pathways. In vascular cells, diverse extracellular signals such as TNF-α mediate NF-κB activation to initiate inflammatory gene expression involved in vascular inflammation (Brasier, 2010). Numerous reports support aberrant vascular inflammation as a major factor in the aggravation of atherosclerosis (Galkina & Ley, 2009; Geovanini & Libby, 2018). In the initiation of atherosclerotic lesion, vascular inflammation can promote *VCAM-1* gene expression via NF-κB in the cells of the vessel wall (Cybulsky et al., 2001). TNF-α-treated endothelial cells can express inflammatory genes, including adhesion molecules, cytokines, and chemokines (Pober, 2002). Thus, inhibiting NF-κB in endothelial cells by nutraceuticals could ameliorate atherosclerosis progression.

Erythorbyl laurate (EL, 6-*O*-lauroyl-erythorbic acid) is a multifunctional compound with surface active, antioxidant, and antimicrobial properties. EL can be produced via lipase-catalyzed esterification of erythorbic acid, a stereoisomer of L-ascorbic acid (vitamin C), and lauric acid, a saturated fatty acid with a 12-carbon chain (Park, Lee, Sung, Lee, & Chang, 2011). The amphiphilic properties of the hydrophilic head group of erythorbic acid and the lipophilic tail group of lauric acid allow it to have interfacial properties, such as foaming ability and emulsifying properties in oil-in-water emulsions (Park et al., 2017). EL demonstrated free radical scavenging activity, including $ABTS^{+}$ and DPPH radicals, and retarded the formation of lipid peroxides in oil-in-water emulsions. EL also exhibited both bacteriostatic and bactericidal effects on Gram-positive bacteria by damaging the bacterial cell membrane (Park et al., 2018). These features make EL a promising candidate as a multifunctional additive for foods and pharmaceuticals. After consumption, EL may be hydrolyzed by pancreatic lipases during digestion, producing erythorbic and lauric acid, which are considered as generally recognized as safe GRAS ingredients. These observations EL may be used as a functional ingredient, without adverse effects or safety concerns.

The aim of the present study was to evaluate the anti-inflammatory effects and underlying molecular targets of EL *in vitro* and *in vivo*. Based on various analyses, we concluded that EL could be a promising anti-atherosclerosis nutraceutical.

2. Materials and methods

2.1. Materials

Human umbilical vein endothelial cells (HUVECs) and monocyte THP-1 cells were purchased from Lonza (Walkersville, MD, USA) and the Korean Cell Line Bank (Seoul, Korea), respectively. Chemical reagents were purchased from Sigma–Aldrich (St Louis, MO, USA). RPMI 1640, penicillin–streptomycin, and fetal bovine serum (FBS) were obtained from Thermo Scientific HyClone (Logan, UT, USA). Recombinant human tumor necrosis factor-alpha (TNF-α) was provided by BD Pharmingen (San Diego, CA, USA). The antibodies against VCAM-1, F4/80, α-tubulin and β-actin were purchased from Santa Cruz Biotech (Santa Cruz, CA, USA). The antibodies against VCAM-1, inhibitor of NF-κB subunit α (IKKα), IKKβ, phospho-IKKα/β (Ser176/180), NF-κB p65, phospho-NF-κB p65 (Ser536), IκBα, phospho-IκB-α (Ser32), and NF-κB1 p105/p50 were purchased from Cell Signaling Biotechnology (Beverly, MA, USA). The antibody against mouse anti-lamin B2 was purchased from EMD Millipore Corporation (Temecula, CA, USA). Alexa Fluor™ 488 goat anti-rat IgG (H + L) secondary antibody was purchased from Thermo Fisher Scientific Inc., (Eugene, Oregon, USA).

2.2. Synthesis of erythorbyl laurate

Erythorbic acid (≥99.0%) and lauric acid (≥99.0%) were purchased from Sigma–Aldrich (St. Louis, MO, USA). Novozym 435, the immobilized lipase from *Candida antarctica*, with a catalytic activity of 7000 PLU/g (1 PLU is the amount of enzyme activity generating 1 μmol of propyl laurate per min at 60 °C) was kindly provided Novozymes (Bagsvaerd, Denmark). EL was produced via lipase-catalyzed esterification of erythorbic acid with lauric acid in a gas-solid-liquid multiphase reaction system (Yu, Lee, Shin, Park, & Chang, 2019). Lauric acid (85.9 mmol) was added into the reaction vessel and melted for 20 min at 60 °C with N_2 gas sparging at a flow rate of 2.0 mL/min. Erythorbic acid (42.93 mmol) and the immobilized lipase (2.4 g; 16,800 PLU) were then added into the vessel. After reaction for 72 h, the reaction mixture was obtained by filtration through a porous glass filter on the reaction vessel with a vacuum pump. EL was purified by solvent-separation, and the purity was determined by quantitative HPLC analysis (LC-2002; Jasco, Tokyo, Japan) with a C18 reverse-phase column (5 μm, 4.6 × 150 mm) and an ultraviolet detector (UV-2075; Jasco).

2.3. Cell culture

HUVECs (1×10^5 cells/mL) were cultured in Endothelial Cell Growth Basal Medium-2 (EBM-2) culture medium supplemented with EGM-2 Single Quots (hEGF, hydrocortisone, FBS, VEGF, hFGF-B, R3-IGF-1, ascorbic acid, GA-1000, heparin) (Lonza). THP-1 cells were grown in RPMI-1640 medium supplemented with 10% FBS and 2-mercaptoethanol to a final concentration of 0.05 mM. To assess cell viability, HUVECs (1×10^5 cells/mL) were seeded in 96-well plates and incubated at 37 °C in a 5% CO_2 incubator. After the cells were treated with the EL, 20 μL of MTS reagent (Promega, Madison, WI, USA) was added to each well. After 1 h of incubation, absorbance levels of formazan at 490 and 690 nm were measured using a microplate reader (Bio-Rad Inc., Hercules, CA, USA).

2.4. Monocyte–endothelial cell adhesion assay

The monocyte–endothelial cell adhesion assay was performed as described previously. THP-1 cells (5×10^5 cells/mL) were incubated with 2 μM calcein AM (Sigma) for 15 min at 37 °C in PBS. HUVECs (3×10^5 cells/mL) were seeded into 96-well plates and incubated for 24 h to obtain confluent monolayers. Then, HUVECs were treated with various concentrations of erythorbic laurate (EL) at 37 °C for 1 h and stimulated with 10 ng/mL TNF-α for 5 h prior to the adhesion assay. Fluorescently labeled THP-1 cells were added to the activated HUVECs, and the plates were incubated for an additional 1 h. After washing out the unbound THP-1 cells with PBS three times, monocyte adhesion was measured by fluorescent intensity using a fluorescent plate reader (SpectraMax M2e; Molecular Devices Corporation, Sunnyvale, CA, USA) at excitation and emission wavelengths of 485 and 538 nm, respectively. The attachment of THP-1 cells was confirmed with a fluorescent microscope (Nikon Eclipse Ti-S, Tokyo, Japan), and images were analyzed using MetaMorph software (Molecular Devices, Danville, PA, USA).

2.5. NF-κB promoter assay

To evaluate the effect of EL on NF-κB promoter activity, we constructed a pGreenFire (pGF1) vector containing the NF-κB promoter. For stable expression of pGF1 with the NF-κB promoter, 293 T cells were transfected with the pGF1 plasmid using Lipofectamine (Thermo Fisher Scientific, MA, USA), following the manufacturer's instructions. The transfection medium was changed 4 h after the transfection, and the cells were cultured for an additional 36 h. Virus particles were harvested by filtration through a 0.45-μm syringe filter, then combined with 1 mg/mL polybrene (Millipore), and used to infect the HUVECs for 24 h. The cell culture medium was replaced with fresh medium, and the cells were further cultured for 24 h prior to selection with puromycin (1 μg/mL) for 36 h. Selected HUVECs (8×10^3 cells/mL) were seeded into 96-well plates, which were incubated at 37 °C in a 5% CO_2 incubator. When the cells reached 80–90% confluence, they were treated with EL for 1 h prior to treatment with 10 ng/mL TNF-α and then incubated for 5 h. The cells were lysed with 100 μL of lysis buffer (0.1 M potassium phosphate buffer [pH 7.8], 1% Triton X-100, 1 mM dithiothreitol, and 2 mM ethylenediaminetetraacetic acid), after which luciferase activity was measured using a luminometer (SpectraMax L; Molecular Devices). Beetle luciferin potassium salt (Promega) was used as a substrate for luciferase.

2.6. Western blot assay

For *in vitro* Western blot assays, HUVECs (2×10^5 cells/mL) were seeded in 10 cm dishes for 24 h. The cells were then treated with EL for 1 h and treated with 10 ng/mL of TNF-α for a specific duration. After incubation, the cells were collected and washed twice with cold PBS before lysis in Cell Lysis Buffer (Cell Signaling Biotechnology, Beverly, MA, USA) and maintained on ice for 30 min. The protein lysate was obtained via centrifugation, and protein concentration was determined using a DC Protein Assay kit (Bio-Rad Laboratories) following the manufacturer's instructions. The lysate was separated by 10% SDS–PAGE and transferred to a polyvinylidene difluoride (PVDF) membrane (Millipore, Immobilon®-P transfer membrane). After transfer, the membranes were incubated with the specific primary antibodies at 4 °C overnight. Protein bands were visualized using a chemiluminescence detection kit (ATTO, Tokyo, Japan) after hybridization with a horseradish peroxidase (HRP)-conjugated secondary antibody.

2.7. Cytoplasmic and nuclear fractionation

HUVECs (2×10^6 cells/mL) were seeded in 10-cm dishes and incubated at 37 °C for 24 h in a 5% CO_2 incubator. The medium was replaced with EL-containing media for 1 h. The cells were then treated with 10 ng/mL TNF-α for 30 min. After incubation, the cells were collected and washed twice with cold PBS. Nuclear protein extraction was performed with NE-PER nuclear and cytoplasmic extraction reagents (Thermo Scientific, Rockford, IL, USA) according to the manufacturer's protocol.

2.8. Total RNA isolation and quantitative real-time reverse transcription–polymerase chain reaction (qRT–PCR) analysis

Total RNA was isolated using an RNeasy® mini kit (Qiagen, Valencia, CA, USA) according to the manufacturer's instructions. The RNA was reverse transcribed with the ReverTra Ace® qPCR RT master mix (Toyobo, Osaka, Japan). First-strand cDNA was prepared from 500 ng of total RNA. The real-time PCR reaction was performed in a reaction volume of 20 μL, containing 1 μg of cDNA, 1 μM of each primer (Table S1), and the Power SYBR® Green PCR master mix (Applied Biosystems, Carlsbad, CA, USA). Thermal cycling was carried out in a StepOnePlus real-time PCR system (Applied Biosystems) at 95 °C for 5 min, followed by 40 cycles of denaturation at 95 °C for 5 s and annealing/elongation at 60 °C for 10 s. Gene expression levels were normalized to that of the glyceraldehyde 3-phosphate dehydrogenase (*GAPDH*) housekeeping gene. The relative gene expression values in treated cells, calculated using the $2^{-\Delta\Delta CT}$ method, are reported as fold changes relative to those of the control cells.

2.9. Animals and experiments design

All animals received humane care in accordance with the guidelines for animal use and care of the Kyungpook National University Institutional Animal Care and Use Committee (IACUC), and the study protocol (KNU-2020-0044) was approved. Ten-week-old male C57BL/6 mice were purchased from Central Lab Animal Inc., (Seoul, Korea). The mice were housed in an air-conditioned room (23 °C ± 2 °C) under a 12-h light/dark cycle. The animals were allowed access to food and tap water *ad libitum*. Twenty-five mice were randomly allocated to five groups (five mice per group): (i) control group (normal); (ii) TNF-α-treated group; (iii) TNF-α- and EL (20 mg/kg body weight/day)-treated group; (iv) TNF-α- and EL (100 mg/kg/day)-treated group; and (v) TNF-α- and bamboo leaf extract (BLE; 100 mg/kg/day)-treated group. The mice in the EL (20 or 100 mg/kg/day)- and BLE (100 mg/kg/day)-treated groups were orally administered with the extracts for 3 days. Starting 1 h after the last oral administration, the mice were induced with an intraperitoneal (i.p.) injection of TNF-α at 25 μg/kg daily for seven consecutive days. The control mice received an i.p. injection of PBS during the same period. Bamboo (*Phyllostachys pubescens*) leaves were extracted as described previously and used as a positive control.

2.10. Immunofluorescence analysis in mouse aorta

Mouse hearts and aorta samples were embedded in frozen section compound (FSC 22; Leica Microsystems, USA) and serially sectioned at 10-μm thickness with a CM1850 cryostat (Leica, Nussloch, Germany). After washing, the sections were incubated with 5% goat serum for 1 h at room temperature to block nonspecific binding. The sections were then incubated with primary antibodies at 4 °C overnight. After washing, the sections were further incubated with an Alexa Fluor™ 488 or Alexa Fluor™ 647 goat anti-mouse IgG (H + L) secondary antibody for 1 h at room temperature. Coverslips were then dried, mounted onto slides, and Vectashield with 4′,6-diamidino-2-phenylindole (Vector Laboratories) was used to stain the nuclei. Images of VCAM-1 and F4/80 mature mouse macrophage and microglial expression markers in the aorta were obtained with a fluorescent microscope (Leica DFC450 C) and analyzed using Leica Application Suite X (Leica Microsystems).

2.11. Statistical analysis

Where appropriate, data are expressed as the mean ± standard error of the mean. Significance of differences was determined using one-way analysis of variance. A p-value of < 0.05 was considered statistically significant.

3. Results

3.1. Erythorbyl laurate lowers TNF-α-induced monocyte adhesion capacity and inhibits VCAM-1 expression

Since abnormal adhesion of monocytes to vascular endothelial cells plays an important role in initiation of vascular inflammation and subsequent atherosclerosis (Galkina & Ley, 2009), we investigated the effect of EL on TNF-α-induced THP-1 adhesion to HUVECs. First, we confirmed that EL (10–40 μM) did not exhibit cytotoxic effects in HUVECs (Fig. 1B). EL suppressed TNF-α-induced THP-1 adhesion to HUVECs in a dose dependent manner (Fig. 1C). In addition, EL significantly suppressed TNF-α-induced VCAM-1 expression in HUVECs

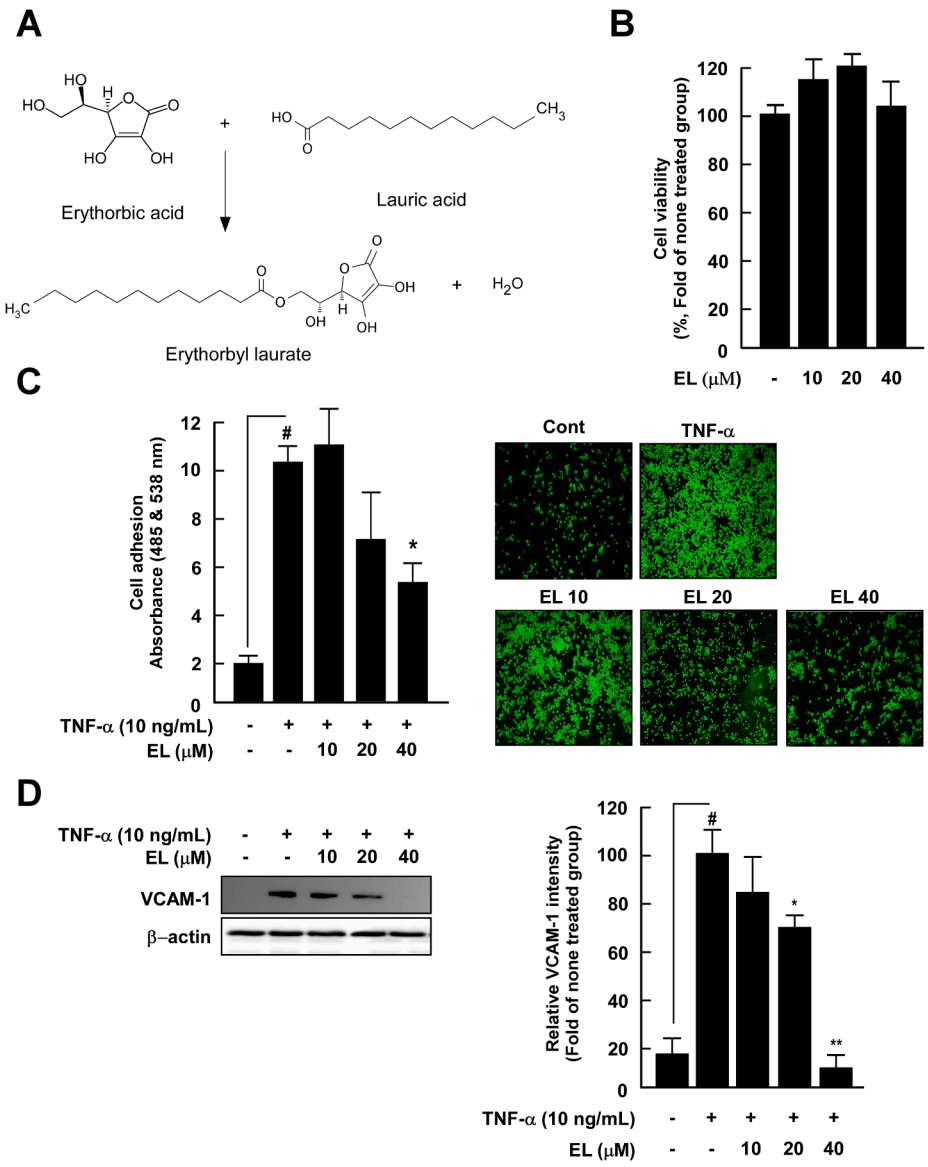

Fig. 1. Erythorvyl laurate (EL) lowers TNF-α-induced adhesion capacity and inhibits VCAM-1 expression in HUVECs. (A) EL is lipase-catalyzed esterification form between erythorbic and lauric acid. (B) Viability of EL-treated HUVECs. (C) THP-1 cell adhesion to HUVECs after treatment with EL and TNF-α. Fluorescently labeled THP-1 cells assessed by fluorescent microscopy. (D) TNF-α-induced VCAM-1 expression in HUVECs after EL and TNF-α treatment. #$p < 0.05$ between the control group and the group exposed to TNF-α alone; *$p < 0.05$ and **$p < 0.01$ between the TNF-α + EL groups and the group exposed to TNF-α alone. Data are presented as the mean ± standard deviation (SD) of three independent experiments.

(Fig. 1D).

3.2. EL inhibits TNF-α-induced NF-κB promoter binding, NF-κB signaling regulator phosphorylation, and p65 nuclear translocation in HUVECs

As activated NF-κB plays a crucial role in the interaction between THP-1 and HUVECs through VCAM-1 expression in vascular endothelial cells (Cybulsky et al., 2001), we examined whether EL affected NF-κB signaling pathways. We firstly evaluated the effect of EL on NF-κB promoter binding activity using a stably transfected *NF-κB*-luciferase reporter plasmid. The results showed that EL significantly suppressed TNF-α-induced NF-κB promoter binding activity (Fig. 2A). We also observed that EL inhibited upstream phosphorylation of IKK, IκB, and p65 in HUVECs (Fig. 2B). Translocation of p65, a subunit of NF-κB with a transactivation domain, is a key step in the regulation of its transcriptional activity (Li & Verma, 2002). Western blot assays on cytosolic and nuclear cellular fractionations (Fig. 2C) and immunofluorescence (Fig. 2D) demonstrated that EL significantly suppressed TNF-α-induced translocation of p65 from the cytosol to the nucleus in HUVECs.

3.3. EL inhibits TNF-α-induced phosphorylation of MAPKs, Akt, IRAK1, and TAK1 in HUVECs

In addition to NF-κB signaling pathways, MAPK signaling pathways are also involved in vascular inflammation (He et al., 2016). We found that EL inhibited TNF-α-induced phosphorylation of ERK1/2, JNK1/2, and p38 MAPKs (Fig. 3A). To determine whether EL inhibition of endothelial activation is dependent on upstream signaling effectors of MAPKs, we also examined phosphorylation status of Akt, IRAK1, and TAK1. Western blot analysis showed that EL significantly suppressed the TNF-α-induced phosphorylation of Akt at Ser 473 and Thr 308, IRAK1, and TAK1 (Fig. 3B).

3.4. EL inhibits TNF-α-induced expression of inflammatory cytokines

Activated NF-κB promotes the expression of cytokines including IL-1β, IL-6, and TNF-α, and chemokines, such as MCP-1, which exacerbate vascular inflammation (Moss & Ramji, 2016a, 2016b; Tedgui & Mallat, 2006). Quantitative RT-PCR results confirmed that EL significantly suppressed TNF-α-induced *IL1B*, *IL6*, *TNFA*, and *CCL2* mRNA expression in HUVECs (Fig. 4).

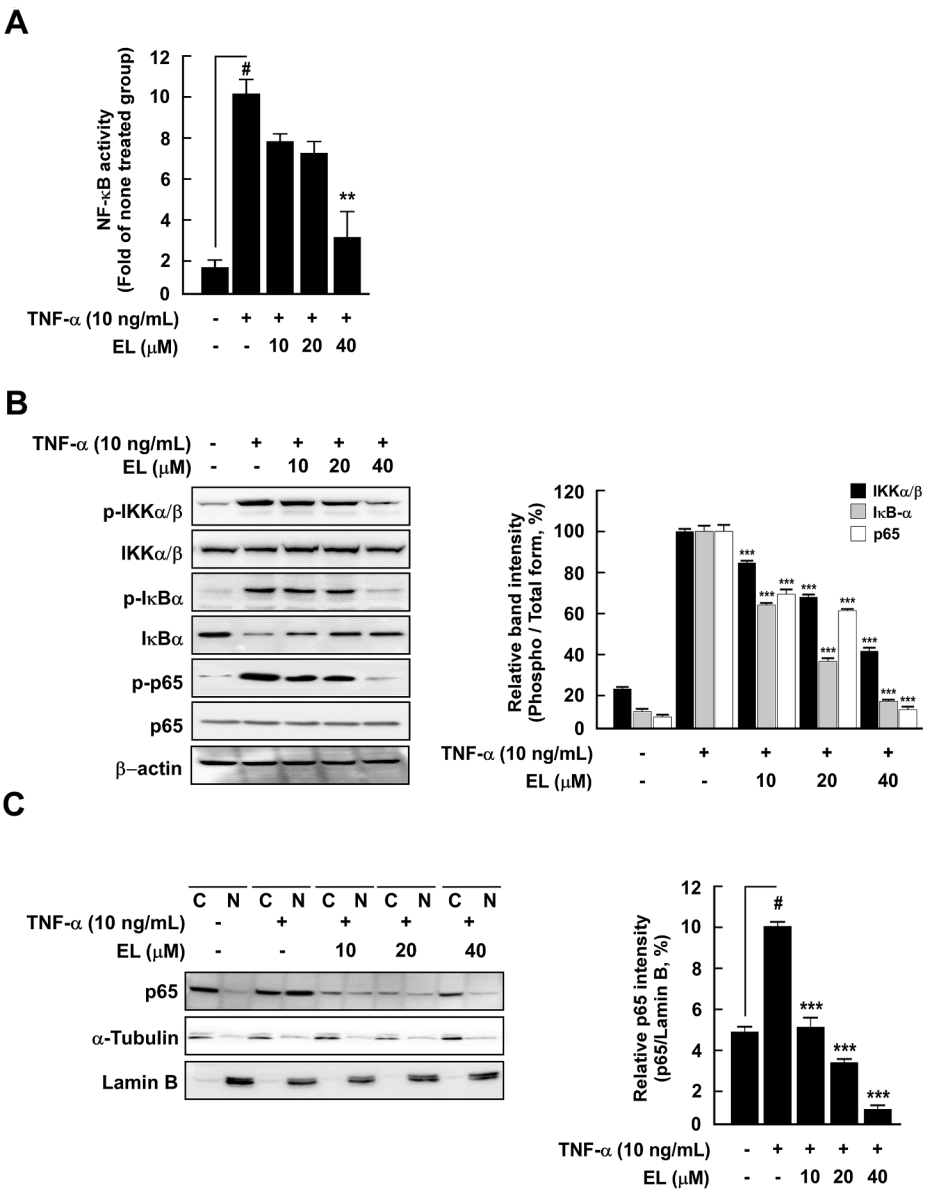

Fig. 2. Erythorbyl laurate (EL) inhibits TNF-α-induced NF-κB promoter binding activity, upstream signaling molecule phosphorylation, and p65 nuclear translocation in HUVECs. (A) NF-κB promoter binding activity. HUVECs were stably transfected with an NF-κB-luciferase reporter plasmid, then treated with EL and TNF-α. (B) Phosphorylated and total IKK, IκB, and p65 levels after EL and TNF-α treatment by Western blotting. (C) p65 cellular localization after EL and TNF-α treatments by Western blotting. α-tubulin and lamin B were used as cytosolic and nucleic protein-loading controls, respectively. (D) p65 cellular localization in HUVECs after treatment with EL and TNF-α by immunofluorescence. p65 and nuclear staining are green and blue, respectively. #$p < 0.05$ between the control group and the group exposed to TNF-α alone; **$p < 0.01$ and ***$p < 0.001$ between the TNF-α + EL groups and the group exposed to TNF-α alone. Data are presented as the mean ± standard deviation (SD) of three independent experiments.

3.5. EL inhibits TNF-α-induced monocyte infiltration into the aortic root and expression of inflammatory cytokines in the aorta

To evaluate the vascular anti-inflammatory effect of EL, we adopted a TNF-α-induced vascular inflammation mouse model and investigated the effect of EL on TNF-α induced monocyte infiltration and VCAM-1 expression in the mouse aortic root. Oral administration of EL suppressed TNF-α-induced monocyte infiltration in the intima in the aortic root (Fig. 5A). Additionally, EL inhibited TNF-α-induced VCAM-1 expression in the aortic root (Fig. 5B). As vascular cytokines are a

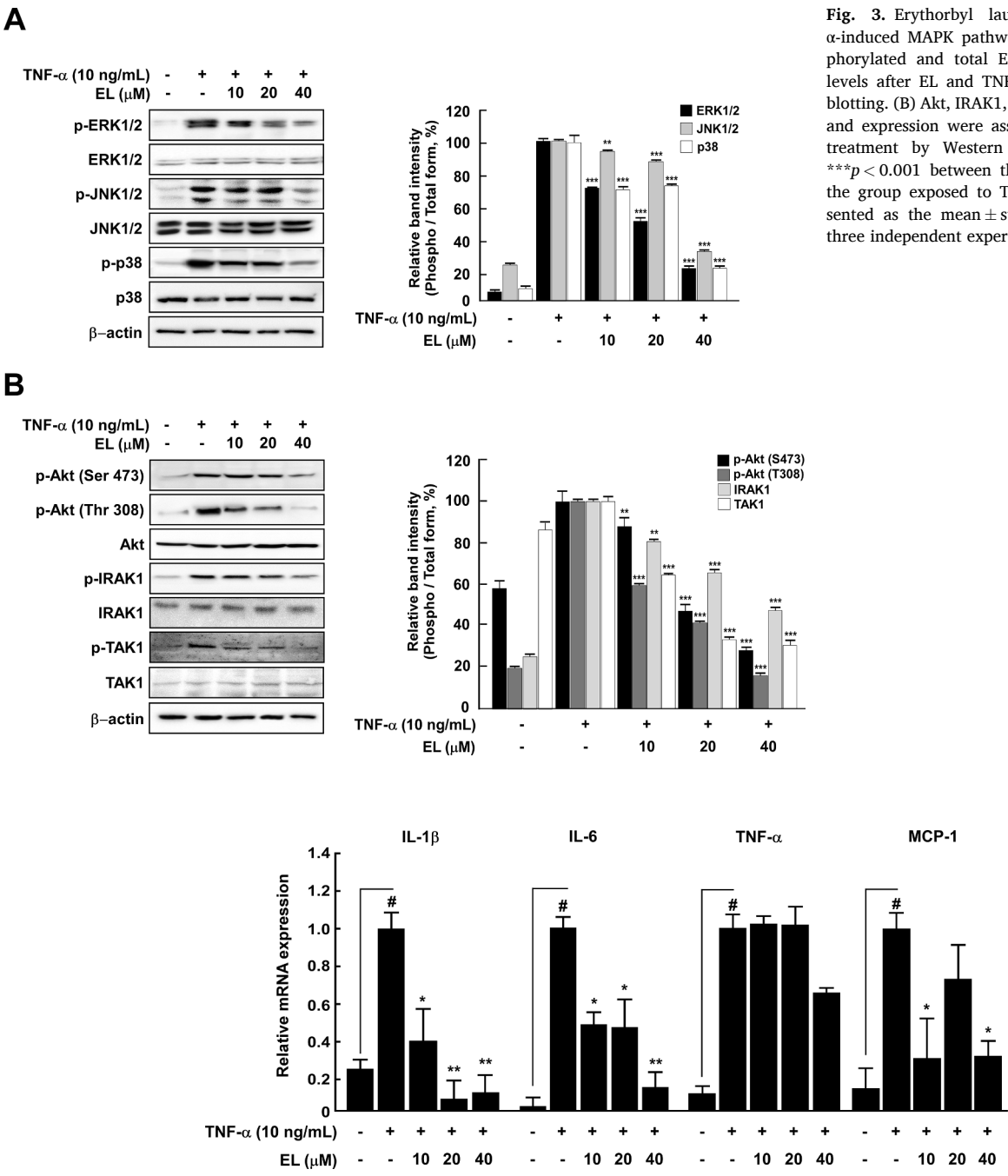

Fig. 3. Erythorbyl laurate (EL) inhibits TNF-α-induced MAPK pathways in HUVECs. (A) Phosphorylated and total ERK1/2, JNK1/2, and p38 levels after EL and TNF-α treatments by Western blotting. (B) Akt, IRAK1, and TAK1 phosphorylation and expression were assessed after EL and TNF-α treatment by Western blotting. $^{**}p < 0.01$ and $^{***}p < 0.001$ between the TNF-α + EL groups and the group exposed to TNF-α alone. Data are presented as the mean ± standard deviation (SD) of three independent experiments.

Fig. 4. Erythorbyl laurate (EL) inhibits the TNF-α-induced expression of proinflammatory cytokines in HUVECs. *IL1B*, *IL6*, *TNFA*, and *CCL2* mRNA expression levels after EL and TNF-α treatment by qRT–PCR. $\#p < 0.05$ between the control group and the group exposed to TNF-α alone; $^{*}p < 0.05$ and $^{**}p < 0.01$ between the TNF-α + EL groups and the group exposed to TNF-α alone. Data are presented as the mean ± standard deviation (SD) of three independent experiments.

representative marker for vascular inflammation (Ramji & Davies, 2015), we evaluated the effect of EL on TNF-α-induced production of proinflammatory cytokines. Quantitative RT-PCR results showed that oral administration of EL significantly suppressed TNF-α-induced *IL6* and *TNFA* mRNA expression in the mouse aorta (Fig. 5C).

4. Discussion

Cardiovascular disease (CVD) produces enormous health burdens globally and is expected to account for more than 23.6 million deaths per year by 2030 (Organization, 2014). Among the various underlying causes of CVDs, atherosclerosis, a systemic disease process within the arterial walls, may contribute to end organ damage including ischemic heart disease and cardiac arrest (Benjamin, Muntner, & Bittencourt, 2019). In a previous study, we proposed that development of atherosclerosis can be divided into four stages: initiation, promotion, progression, and acute events (Kim & Jung, 2020). The early stages of atherosclerosis include initiation and promotion, which involve monocyte recruitment. This occurs via multiple process mediated by the expression of cell adhesion molecules and chemoattractant molecules (Libby, Ridker, & Maseri, 2002). Thus, the early stages should be a primary target for prevent atherosclerosis. A substantial body of experimental evidence demonstrates that TNF-α, a proinflammatory cytokine, induces endothelial cell activation and other inflammatory processes during the early stages of atherosclerosis (Branen et al., 2004; Clausell, Molossi, Sett, & Rabinovitch, 1994). TNF-α-stimulated

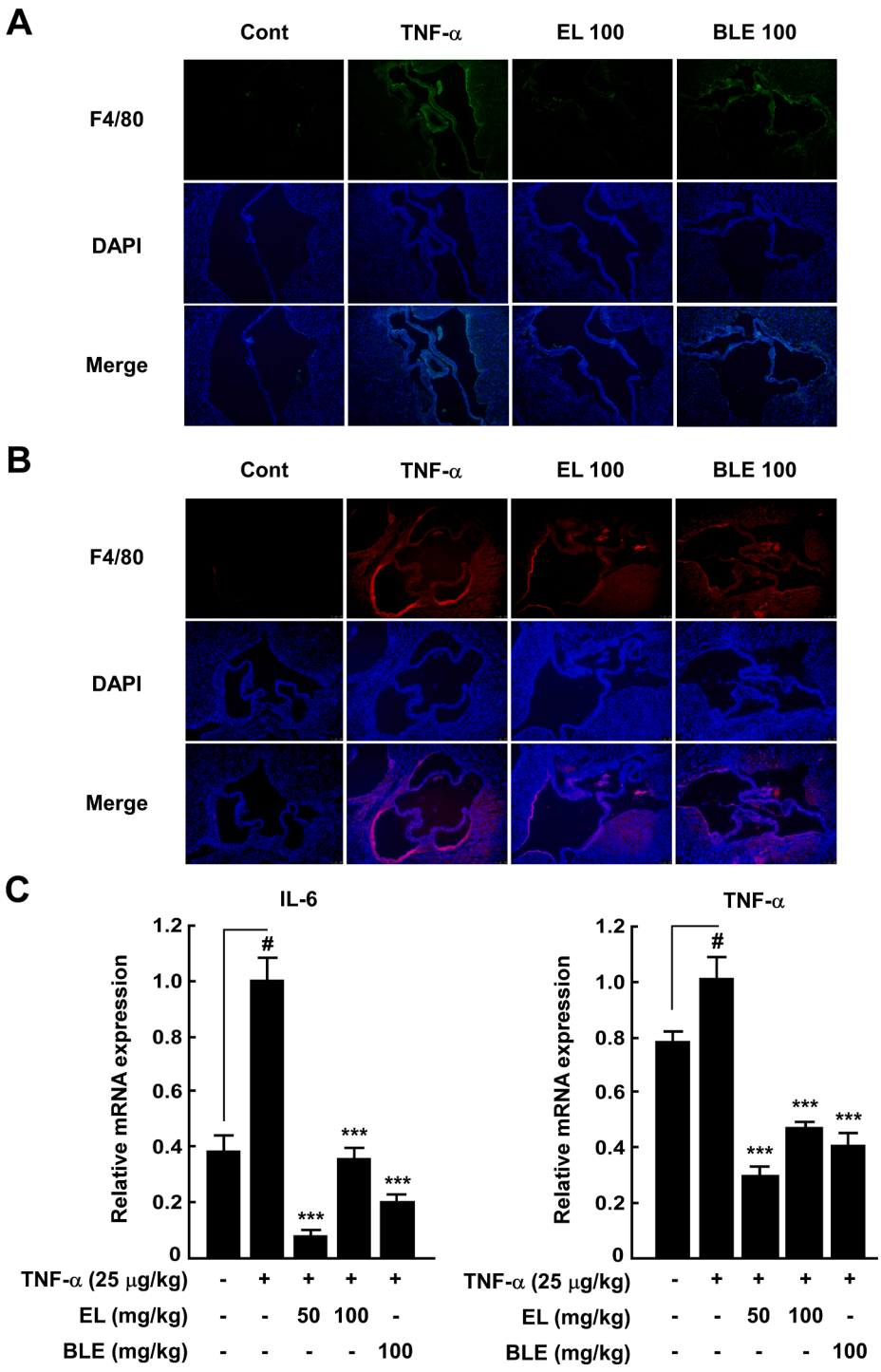

Fig. 5. Erythorbyl laurate (EL) inhibits TNF-α-induced monocyte infiltration into the aortic root and inhibits *IL6* and *TNFA* mRNA expression in the aorta. (A) Monocyte infiltration into the C57Bl/6 mice aortic root following EL and TNF-α treatment. (B) VCAM-1 expression in the mouse aorta following EL and TNF-α treatment. (C) *IL6* and *TNFA* mRNA expression in the aorta of C57Bl/6 mice following oral EL treatment and TNF-α intraperitoneal injection, by qRT–PCR. $\#p < 0.05$ between the control group and the group exposed to TNF-α alone; $^{***}p < 0.001$ between the TNF-α + EL groups and the group exposed to TNF-α alone. Data are presented as the mean ± standard deviation (SD) of three independent experiments.

endothelial cells display abnormal expression of VCAM-1 in atherosclerotic lesions (Knowles & Maeda, 2000; Richardson, Hadcock, DeReske, & Cybulsky, 1994).

Many researchers have participated in the development of functional food additives for the prevention of arteriosclerosis and have shown materials derived from natural products can suppress vascular inflammation (Hur & Lee, 2017; Jeon, Kim, & Kim, 2017). However, nutraceuticals that can prevent cardiovascular disease by suppressing vascular inflammation still needed to be developed. As a novel nutraceutical candidate, EL is synthesized form of erythorbic acid with lauric acid through an esterification reaction by immobilized lipase (Park et al., 2018). In a previous report, the effect of erythorbic acid and lauric acid exhibited interfacial and antibacterial properties, which provided the basis for the use of food additives such as emulsifiers in lipid-based foods. However, the effect of EL on vascular inflammation and its mechanism of action remained unclear. Therefore, we investigated the effect of EL on TNF-α-induced vascular inflammation and its signaling networks in HUVECs. We found that EL significantly suppressed TNF-α-induced monocyte adhesion to HUVECs and VCAM-1 expression in HUVECs. In our previous study (Ha et al., 2018), we showed that *Lespedeza cuneata* extract suppressed TNF-α-induced interactions between monocytes and HUVECs via VCAM-1 inhibition, and these results were consistent with our *in vivo* results from this study. Therefore, EL and *L. cuneata* extract exert similar protective effects on vascular

inflammation both *in vitro* and *in vivo*.

NF-κB is a critical transcription factor in the expression of VCAM-1 and other inflammatory cytokines that initiate monocyte infiltration into the intima during the early stages of atherosclerosis (Ronald, Ionescu, Rogers, & Sandig, 2001). Several studies have demonstrated that inhibition of NF-κB signaling in endothelial cells has an anti-atherosclerotic effect via downregulation of adhesion molecules and other inflammatory mediators (Brand et al., 1996; Gareus et al., 2008). We observed that EL inhibited TNF-α-induced phosphorylation of NF-κB pathway mediators such as p65, IKK, and IκB. Additionally, EL also suppressed TNF-α-induced p65 nuclear translocation. As translocation of NF-κB from the cytosol to the nucleus is an essential step in the regulation of transcription of target genes such as *VCAM-1*, suppression of this translocation by EL describes the mechanism of EL inhibition of TNF-α-induced VCAM-1 expression and monocyte adhesion capacity.

TNF-α activates not only NF-κB signaling but also MAPK signaling pathways (Sabio & Davis, 2014; Varfolomeev & Vucic, 2018). In general, JNK and p38 are known as stress-activated MAP kinases, whereas ERK is activated by mitogens and differentiation (Zhang & Liu, 2002). Thus, activated MAPKs are critical signaling molecules in TNF-α-induced vascular inflammation. Therefore, once natural materials regulate MAPK phosphorylation and associated signaling cascades, it suggests a promising strategy for the development of nutraceuticals to combat vascular inflammation. As evidence of this, several studies have demonstrated the downregulation of TNF-α-mediated MAPK signaling, such as MAPK/Akt/NF-κB by *diosgenin* and MAPK phosphorylation by *wogonin*. It is suggested that the inhibition of these signaling processes is critical for the suppression of vascular inflammation (Choi et al., 2010; Lee et al., 2006). Our Western blot analyses confirmed that EL reduced TNF-α-induced phosphorylation of MAPKs as well as IKKα/β, IκB, and p65 in HUVECs. Therefore, inhibition of MAPK- and NF-κB-related molecules may also be related the reduction in monocyte adhesion to vascular endothelial cells.

Based on these results, we investigated molecules which have been shown to regulate both NF-κB and MAPK signaling pathways triggered by TNF-α. Previously published reports have shown that TGF-β-activated kinase 1 (TAK1), a member of the MAPK kinase kinase (MAP3K) family also called MAP3K7, can be activated by TNF-α or various other stimuli (Huang, Shi, & Chi, 2009; Takaesu et al., 2003). TAK1 has a major role in vascular disease; it responds to exogenous stress conditions by regulating proinflammatory signaling pathways (Song et al., 2014). TAK1 is also regulated through specific binding proteins, such as TAK1-binding protein (TAB) 1, TAB 2, and TAB 3 (Aashaq, Batool, & Andrabi, 2019), and can subsequently activate MAPK cascades, such as MKK3/6 and MKK4/7, and NF-κB, such as IKK (Mihaly, Ninomiya-Tsuji, & Morioka, 2014). Interestingly, EL suppressed TNF-α-induced phosphorylation of TAK1. In addition to TAK1, Interleukin-1 receptor associated kinase-1 (IRAK-1) was phosphorylated upon TNF-α treatment and inhibited by pre-treatment with EL. We hypothesized that TAK1 and IRAK1 act upstream of TNF-α-induced MAPKs or/and NF-κB; however, further studies including siRNA knockdown of TAK1 and IRAK1 will need to be performed.

These accumulated results indicate that EL has an inhibitory effect on TNF-α-induced VCAM-1 expression and subsequent monocyte adhesion to vascular endothelium via regulation of MAPK/Akt/NF-κB signaling in HUVECs. To confirm the direct vascular anti-inflammatory effect of EL, we further performed *in vivo* experiments in mice. In our previous study, we observed that i.p. injection of TNF-α results in vascular inflammation, including monocyte infiltration into the intima and upregulation of inflammatory cytokines including *IL1*, *IL6*, and *TNFA*. Using this model, we found that oral administration of EL prevents TNF-α-induced upregulation of monocyte infiltration into the intima of the aortic root. Additionally, oral administration of EL also suppressed VCAM-1 expression in the aortic root. Quantitative RT-PCR of mouse aorta-derived mRNAs showed that EL significantly suppressed TNF-α-induced *IL6* and *TNFA* mRNA expression. Since the aortic root is susceptible to vascular inflammation and subsequent formation of lipid plaques, inhibition of monocyte infiltration into the intima of blood vessels can prevent monocyte-induced foam cell formation and atherosclerosis. In conclusion, EL reduces abnormal adhesion of monocytes to endothelial cells and infiltration of monocytes via regulation of VCAM-1 expression and phosphorylated TAK1. Collectively, the results of this study provide evidence that EL possesses anti-atherosclerotic properties *in vitro* and *in vivo*.

5. Conclusions

In this study, we confirmed that EL suppresses TNF-α-induced monocyte adhesion to the vascular endothelium, as well as expression of inflammatory cytokines *IL6* and *TNFA* both *in vitro* and *in vivo*. These result from suppression of NF-κB signaling via p65 nuclear translocation and inhibition of MAPK phosphorylation. Our results indicate that EL has promising anti-inflammatory properties that can inhibit monocyte adhesion to vascular endothelium and reduce expression of inflammatory cytokines.

6. Ethics statements

All animals received humane care in accordance with the guidelines for animal use and care of the Kyungpook National University Institutional Animal Care and Use Committee (IACUC), and the study protocol (KNU-2020-0044) was approved.

CRediT authorship contribution statement

Su Jeong Ha: Software, Validation, Formal analysis, Data curation, Visualization. **Min Jeong Kim:** Validation, Formal analysis, Writing - original draft, Visualization. **Joon Park:** Validation, Investigation. **Hyun-Wook Choi:** Writing - review & editing. **Hyunjong Yu:** Resources, Investigation. **Pahn-Shick Chang:** Investigation, Writing - review & editing. **Sung Keun Jung:** Conceptualization, Methodology, Investigation, Resources, Writing - review & editing, Supervision, Project administration, Funding acquisition.

Declaration of Competing Interest

The authors declare that they have no known competing financial interests or personal relationships that could have appeared to influence the work reported in this paper.

Acknowledgements

This project was supported by the Basic Science Research Program through the National Research Foundation of Korea (NRF), which is funded by the Ministry of Education (2018R1D1A1B07050031).

Appendix A. Supplementary data

Supplementary data to this article can be found online at https://doi.org/10.1016/j.jff.2021.104428.

References

Aashaq, S., Batool, A., & Andrabi, K. I. (2019). TAK1 mediates convergence of cellular signals for death and survival. *Apoptosis, 24*(1–2), 3–20. https://doi.org/10.1007/s10495-018-1490-7.

Alwan, A. (2011). *Global status report on noncommunicable diseases 2010*. World Health Organization.

Benjamin, E. J., Muntner, P., & Bittencourt, M. S. (2019). Heart disease and stroke statistics-2019 update: A report from the American Heart Association. *Circulation, 139*(10), e56–e528.

Brand, K., Page, S., Rogler, G., Bartsch, A., Brandl, R., Knuechel, R., … Neumeier, D. (1996). Activated transcription factor nuclear factor-kappa B is present in the atherosclerotic lesion. *The Journal of Clinical Investigation, 97*(7), 1715–1722.

Branen, L., Hovgaard, L., Nitulescu, M., Bengtsson, E., Nilsson, J., & Jovinge, S. (2004). Inhibition of tumor necrosis factor-alpha reduces atherosclerosis in apolipoprotein E knockout mice. *Arteriosclerosis, Thrombosis, and Vascular Biology, 24*(11), 2137–2142. https://doi.org/10.1161/01.ATV.0000143933.20616.1b.

Brasier, A. R. (2010). The nuclear factor-κB–interleukin-6 signalling pathway mediating vascular inflammation. *Cardiovascular Research, 86*(2), 211–218.

Choi, K.-W., Park, H.-J., Jung, D. H., Kim, T.-W., Park, Y.-M., Kim, B.-O., … Rhee, D.-K. (2010). Inhibition of TNF-α-induced adhesion molecule expression by diosgenin in mouse vascular smooth muscle cells via downregulation of the MAPK, Akt and NF-κB signaling pathways. *Vascular Pharmacology, 53*(5–6), 273–280.

Clausell, N., Molossi, S., Sett, S., & Rabinovitch, M. (1994). In vivo blockade of tumor necrosis factor-alpha in cholesterol-fed rabbits after cardiac transplant inhibits acute coronary artery neointimal formation. *Circulation, 89*(6), 2768–2779. https://doi.org/10.1161/01.cir.89.6.2768.

Cybulsky, M. I., Iiyama, K., Li, H., Zhu, S., Chen, M., Iiyama, M., … Milstone, D. S. (2001). A major role for VCAM-1, but not ICAM-1, in early atherosclerosis. *The Journal of Clinical Investigation, 107*(10), 1255–1262.

Galkina, E., & Ley, K. (2009). Immune and inflammatory mechanisms of atherosclerosis. *Annual Review of Immunology, 27*.

Gareus, R., Kotsaki, E., Xanthoulea, S., van der Made, I., Gijbels, M. J., Kardakaris, R., … Pasparakis, M. (2008). Endothelial cell-specific NF-κB inhibition protects mice from atherosclerosis. *Cell metabolism, 8*(5), 372–383.

Geovanini, G. R., & Libby, P. (2018). Atherosclerosis and inflammation: Overview and updates. *Clinical Science, 132*(12), 1243–1252.

Ha, S. J., Lee, J., Song, K. M., Kim, Y. H., Lee, N. H., Kim, Y. E., & Jung, S. K. (2018). Ultrasonicated Lespedeza cuneata extract prevents TNF-alpha-induced early atherosclerosis in vitro and in vivo. *Food & Function, 9*(4), 2090–2101. https://doi.org/10.1039/c7fo01666b.

Hansson, G. K. (2005). Inflammation, atherosclerosis, and coronary artery disease. *New England Journal of Medicine, 352*(16), 1685–1695.

He, H., Guo, F., Li, Y., Saaoud, F., Kimmis, B. D., Sandhu, J., … Papasian, C. J. (2016). Adiporedoxin suppresses endothelial activation via inhibiting MAPK and NF-κB signaling. *Scientific Reports, 6*(1), 1–10.

Huang, G., Shi, L. Z., & Chi, H. (2009). Regulation of JNK and p38 MAPK in the immune system: Signal integration, propagation and termination. *Cytokine, 48*(3), 161–169.

Hur, H. J., & Lee, A. S. (2017). Protective effect of allium tuberosum extract on vascular inflammation in tumor necrosis factor-α-induced human vascular endothelial cells. *Journal of Cancer Prevention, 22*(4), 228.

Jeon, D., Kim, S. J., & Kim, H. S. (2017). Anti-inflammatory evaluation of the methanolic extract of Taraxacum officinale in LPS-stimulated human umbilical vein endothelial cells. *BMC Complementary and Alternative Medicine, 17*(1), 1–10.

Kim, M. J., & Jung, S. K. (2020). Nutraceuticals for prevention of atherosclerosis: Targeting monocyte infiltration to the vascular endothelium. *Journal of Food Biochemistry*, e13200. https://doi.org/10.1111/jfbc.13200.

Knowles, J. W., & Maeda, N. (2000). Genetic modifiers of atherosclerosis in mice. *Arteriosclerosis, Thrombosis, and Vascular Biology, 20*(11), 2336–2345. https://doi.org/10.1161/01.atv.20.11.2336.

Lee, S.-O., Jeong, Y.-J., Yu, M. H., Lee, J.-W., Hwangbo, M. H., Kim, C.-H., & Lee, I.-S. (2006). Wogonin suppresses TNF-α-induced MMP-9 expression by blocking the NF-κB activation via MAPK signaling pathways in human aortic smooth muscle cells. *Biochemical and Biophysical Research Communications, 351*(1), 118–125.

Li, Q., & Verma, I. M. (2002). NF-κB regulation in the immune system. *Nature Reviews Immunology, 2*(10), 725–734.

Libby, P., Ridker, P. M., & Maseri, A. (2002). Inflammation and atherosclerosis. *Circulation, 105*(9), 1135–1143.

Mihaly, S. R., Ninomiya-Tsuji, J., & Morioka, S. (2014). TAK1 control of cell death. *Cell Death & Differentiation, 21*(11), 1667–1676.

Moss, J. W., & Ramji, D. P. (2016a). Cytokines: Roles in atherosclerosis disease progression and potential therapeutic targets. *Future Medicinal Chemistry, 8*(11), 1317–1330.

Moss, J. W., & Ramji, D. P. (2016b). Nutraceutical therapies for atherosclerosis. *Nature Reviews Cardiology, 13*(9), 513–532. https://doi.org/10.1038/nrcardio.2016.103.

Organization, W. H. (2014). *Global status report on noncommunicable diseases 2014*. World Health Organization.

Park, K.-M., Jo, S.-K., Yu, H., Park, J.-Y., Choi, S. J., Lee, C. J., & Chang, P.-S. (2018). Erythorbyl laurate as a potential food additive with multi-functionalities: Antibacterial activity and mode of action. *Food Control, 86*, 138–145. https://doi.org/10.1016/j.foodcont.2017.11.008.

Park, K.-M., Lee, D. E., Sung, H., Lee, J., & Chang, P.-S. (2011). Lipase-catalysed synthesis of erythorbyl laurate in acetonitrile. *Food Chemistry, 129*(1), 59–63. https://doi.org/10.1016/j.foodchem.2011.04.019.

Park, K. M., Lee, M. J., Jo, S. K., Choi, S. J., Lee, J., & Chang, P. S. (2017). Erythorbyl laurate as a potential food additive with multi-functionalities: Interfacial characteristics and antioxidant activity. *Food Chemistry, 215*, 101–107. https://doi.org/10.1016/j.foodchem.2016.07.174.

Pober, J. S. (2002). Endothelial activation: Intracellular signaling pathways. *Arthritis Research & Therapy, 4*(3), S109.

Ramji, D. P., & Davies, T. S. (2015). Cytokines in atherosclerosis: Key players in all stages of disease and promising therapeutic targets. *Cytokine & Growth Factor Reviews, 26*(6), 673–685.

Richardson, M., Hadcock, S. J., DeReske, M., & Cybulsky, M. I. (1994). Increased expression in vivo of VCAM-1 and E-selectin by the aortic endothelium of normolipemic and hyperlipemic diabetic rabbits. *Arteriosclerosis and Thrombosis, 14*(5), 760–769. https://doi.org/10.1161/01.atv.14.5.760.

Ronald, J. A., Ionescu, C. V., Rogers, K. A., & Sandig, M. (2001). Differential regulation of transendothelial migration of THP-1 cells by ICAM-1/LFA-1 and VCAM-1/VLA-4. *Journal of Leukocyte Biology, 70*(4), 601–609.

Sabio, G., & Davis, R. J. (2014). TNF and MAP kinase signalling pathways. *Paper presented at the Seminars in immunology*.

Sievenpiper, J. L., & Lavie, C. J. (2018). Dietary prevention of cardiovascular diseases. *Progress in Cardiovascular Diseases, 61*(1), 1–2. https://doi.org/10.1016/j.pcad.2018.05.001.

Song, Z., Zhu, X., Jin, R., Wang, C., Yan, J., Zheng, Q., … Li, G. (2014). Roles of the kinase TAK1 in CD40-mediated effects on vascular oxidative stress and neointima formation after vascular injury. *PLoS ONE, 9*(7), Article e101671. https://doi.org/10.1371/journal.pone.0101671.

Takaesu, G., Surabhi, R. M., Park, K.-J., Ninomiya-Tsuji, J., Matsumoto, K., & Gaynor, R. B. (2003). TAK1 is critical for IκB kinase-mediated activation of the NF-κB pathway. *Journal of Molecular Biology, 326*(1), 105–115.

Tedgui, A., & Mallat, Z. (2006). Cytokines in atherosclerosis: Pathogenic and regulatory pathways. *Physiological Reviews, 86*(2), 515–581.

Varfolomeev, E., & Vucic, D. J. C. (2018). Intracellular regulation of TNF activity in health and disease. *Cytokine, 101*, 26–32.

Yu, H., Lee, M. W., Shin, H., Park, K. M., & Chang, P. S. (2019). Lipase-catalyzed solvent-free synthesis of erythorbyl laurate in a gas-solid-liquid multiphase system. *Food Chemistry, 271*, 445–449. https://doi.org/10.1016/j.foodchem.2018.07.134.

Zhang, W., & Liu, H. T. (2002). MAPK signal pathways in the regulation of cell proliferation in mammalian cells. *Cell Research, 12*(1), 9–18.

Zimmer, S., Grebe, A., & Latz, E. (2015). Danger signaling in atherosclerosis. *Circulation Research, 116*(2), 323–340. https://doi.org/10.1161/CIRCRESAHA.116.301135.